Proceedings of the 2023 Winter Simulation Conference
C. G. Corlu, S. R. Hunter, H. Lam, B. S. Onggo, J. Shortle, and B. Biller, eds.

SEAIRD MODEL TO SIMULATE THE IMPACT OF HUMAN BEHAVIORS

Aidan Fahlman
Gabriel Wainer

Systems and Computer Engineering
Carleton University
1125 Colonel By Dr
Ottawa, ON K1S 5B6, CANADA

2023 Winter Simulation Conference (WSC) | 979-8-3503-6966-3/23/$31.00 ©2023 IEEE | DOI: 10.1109/WSC60868.2023.10408174

ABSTRACT

Compartmental models have been utilized in the study and understanding of the COVID-19 pandemic. Traditional models have been expanded to include geographical level transmission dynamics and new states. Here, we present a model based on Cell-DEVS specifications that can be used to define and study the effects of basic human behavior. We include mask wearing and lockdown fatigue, and an adaptable framework allowing for the rapid prototyping of different diseases and behaviors. We exemplify how to build the model and adapt the attributes using the provinces of Canada as a case study. The results show the effect mask mandates, mask wearing, and lockdown fatigue have on case counts over time.

1 INTRODUCTION

In December 2019 a new infectious disease was identified in Wuhan, China. By the end of January 2020 Canada had its first case of COVID-19 in Toronto, Ontario (Urrutia et al. 2021). Now, in 2023 we are still feeling the effects of COVID-19, many countries still seeing significant cases every day (WHO 2021). Throughout the pandemic there have been different levels of lockdowns, government restrictions, and other rules put in place by government officials. These non-pharmaceutical interventions (NPI) have impact on human behavior and many research efforts showed how long lockdowns caused fatigue, leading to ignore restrictions and reducing lockdown effectiveness (Flaxman et al. 2020; Goldstein et al. 2021; Joshi and Musalem 2021). Mask wearing has been another important focus for researchers. Different types of masks have shown different levels of effectiveness, this combined with mask compliance has shown to make a significant difference on how fast COVID-19 can spread through a population (Grinshpun et al. 2009; Tay et al. 2021; Maged et al. 2022; Rengasamy et al. 2014).

Many of the NPI were evaluated with models of the spread disease. One of such models Kermack and McKendrick (1927) categorizes the population into three "compartments": Susceptible to the disease, Infective (capable of transmitting it), and Recovered (SIR). Simulation results obtained from such models helped officials plan public health measures before the number of cases becomes unmanageable, allowing to evaluate the impact of various NPI on the future spread of the disease (Mader and Rüttenauer 2022). Although there have been many advances in these models, human behavior and its impact have not been studied or modelled as closely. Most compartmental models focus on disease transmission dynamics but fail to incorporate the impact human behavior has on the dynamics. The addition of mask wearing, type, lockdown fatigue, etc. would allow to simulate the impact basic human behaviors would have on disease spread, helping governments and policy-makers to plan and respond to a pandemic better.

Considering these issues, this research focuses on the definition advanced SIR models, specifically a geographical Susceptible-Exposed-Asymptomatic-Infective-Recovered-Deceased (SEAIRD) model whose aim is to incorporate human behavior aspects for COVID-19. Our implementation allows users to run the model at a user-defined region level. The model is designed using the Cell-DEVS formalism (Wainer 2019) and implemented using the Cadmium simulator (Vicino et al. 2019). The model's adaptable framework

allows for accessible rapid-prototyping. We implement mask usage including efficiency, compliance, and behavior around mask usage and lockdown fatigue where a population will suffer from lockdown fatigue over long periods of lockdowns leading to increased disobedience. Users can also input a described group of neighborhoods, allowing for visualization of how a disease might spread through a city, town, or country. We present a case study where the model's neighborhoods are defined as the provinces of Canada. Our results show how different levels of mask usage, mask effectiveness, and lockdown fatigue can result in a change in total case counts over time. Our model provides a framework to rapidly prototype disease spread in their neighborhood where asymptomatic infections can be considered and incorporated where necessary.

2 BACKGROUND / RELATED WORK

As discussed earlier, Kermack and McKendrick (1927) introduced the SIR models in which population moves from one compartment to another based on a set of differential equations. Their work was the foundation for many of the SIR-type models that were developed in the years to come, which incorporated more advanced transitions, states, disease and population rules. One common addition to the SIR model was the Deceased (SIRD) compartment where the models population could die after becoming infected (Calafiore et al. 2020). Another common extension is the Exposed state (SEIRD) where the population become exposed to the disease before being infected (Korolev 2021). More advanced models incorporate new states, like Giordano et al. (2020) where Asymptomatic and Quarantine states are added. Potasman (2017) included Diagnosed, Ailing, Recognized, Threatened, Healed and Extinct.

The definition of geographical SIR models allow to use a cell space to represent a geographical regions as large as countries or as small as individual rooms. Early work in this area included a structured epidemic model with geographic mobility (Sattenspiel and Dietz 1995). Recently, Cárdenas et al. (2020) defined a geographical SIR model based on Zhong et al. (2009) using Cell-DEVS (Wainer 2019). The model allows for inputs such as hospital capacities, lockdown correction factors and a Deceased state. The model can also define geographical based disease spread between two regions based on a correlation factor, which allows to link two neighboring cells together based on geographical information such as the shared border length between the two neighborhoods, which can be described as follows:

$$cij = cji = \frac{\frac{z_{ij}}{li} + \frac{z_{ji}}{lj}}{2}$$

This describes the weighted correlation factor C_{ij}, which uses the two values, the shared boundary length between cells i and j (z_{ij}, z_{ji}) in both directions, divided by the total boundary length of both cells i and j (l_i, l_j). This method states that the correlation for i, when moving to j, is the same as j moving to i.

Davidson and Wainer (2021) further extended this model to include the Exposed state better model the transition from susceptible to infected, including incubation rates (SEIRD). An asymptomatic state was added (SEAIRD) to explore how this population would be different than a regular infectious population. We showed how asymptomatic people could move between neighborhoods with less care since they did not know they were infectious and could spread the disease unknowingly (Fahlman et al. 2021).

Since the beginning of the COVID pandemic, mask wearing has been an important topic of discussion. SIR models were developed to explore and implement how mask wearing impacts disease spread. Maged et al. (2022) defined a SEIR model where mask wearing impacted the rate of infection of a population. The study showed how mask compliance and mask effectiveness changed the levels of infection. Many studies shown that mask wearing over time changes depending on government policies, fatigue and behavioral changes; for instance Mohammadi et al. (2022) defined a SEIARL model where a population had the ability to isolate while infectious. In this study real data was used to model the COVID-19 pandemic where different levels of mask compliance and mask efficiency were defined. The model explored how other Non-Pharmaceutical Interventions (NPI's) like mobility impact the spread of COVID-19 as well. Another example of modelling the impact of masks using a modified logistic function is described in Tay et al.

(2021). This model allowed for compliance of masks to change over time based on a logistic function. One setback to these models is that they do not include a method where the mask wearing compliance or efficiency would change dynamically depending on the state of the model.

When a population is under lockdown for a significant amount of time, they will become frustrated and will begin to require human contact; the lack of these interactions is called *lockdown fatigue* (Goldstein et al. 2021). Many models have explored how long periods of lockdowns or heavy government restrictions impacted human behavior. One such study found that lockdown fatigue is an important factor when considering long lockdowns. The study conducted by Joshi and Musalem (2021) found lockdowns lose 30.1% of the mobility reduction achieved within 28 days and 100% of the mobility impact was lost in day 112. The study of length of lockdowns led to an advanced continuous-time Markov chain model with eight states (SEAMHQRD‑V) where lockdown lengths and impact were considered (Oraby et al. 2021). The model found that shorter lockdowns seemed to have a larger relative effect on the total COVID-19 attack rate. The study of lockdown fatigue and lockdown timing is an important factor for policy makers to consider when planning the impact of lockdowns and may help decide whether earlier, shorter lockdowns would be more effective than waiting and having to enact an aggressive long-lasting lockdown.

Our research focuses on geographical models, allowing the definition of models at a regional level which could be a city, town, or country. We build the spatial models using Cell-DEVS (Wainer 2019), which allows defining cell spaces based on DEVS (Zeigler et al. 2000). Cell-DEVS defines n-dimensional cell spaces where each cell is a DEVS atomic model and the cell space is a coupled model, as in Figure 1. When a cell receives an input, the local computing function τ is activated, computing the next state for the cell. We only consider and compute active cells using a continuous time base. If there is a change in the cell's state, the change is transmitted after a time delay d. Cell-DEVS accepts other neighborhoods and irregular topologies as well. Cell-DEVS inherits the modularity and hierarchical modeling ability of DEVS. This allows for models to better interact with other models, tools, datasets, and visualization tools, making it an easy, and efficient method to build complex cellular models.

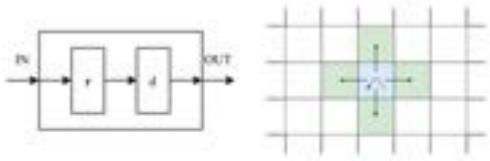

Figure 1: Cell-DEVS model: (left) Atomic cell schematics; (right) 2D Cell-DEVS neighborhood.

There are different simulators to execute Cell-DEVS models (Vicino et al. 2019). In this research, we use the Cadmium tool (Vicino et al. 2019), which allows users to define model inputs using JavaScript Object Notation (JSON), a data format to store and transmit large amounts of human readable data. JSON stores data in key-value pairs allowing for the simple representation of neighborhoods, their attributes, and their relationships. Cadmium allows the user to include complex geographical inputs that load into the model at run time resulting in a flexible model that allows for efficient rapid prototyping.

3 MODELING HUMAN BEHAVIOR IN SEAIRD MODELS

The model in this section includes multiple layers of human behavior (Fahlman et al. 2021). Besides the basic behavior, this model defines individuals including mask wearing compliance, mask types, level of fatigue, as well as disobedience and non-compliance. Figure 2 shows the states included in the model and their respective transitions. A cell's population begins with a fully susceptible population before a disease is introduced. Then, the population in contact with infected individuals become exposed who either become infectious or asymptomatic. The asymptomatic population will eventually recover from the disease as they do not have symptoms, but the infectious population will either move to the recovered state or deceased. The model has the capability for a population to become re-susceptible if needed.

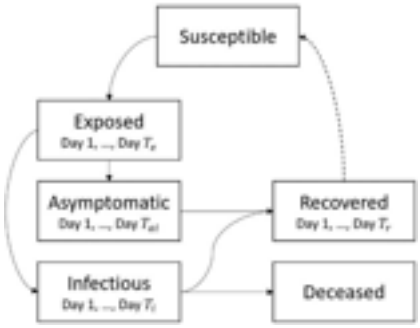

Figure 2: SEAIRD state diagram.

Each state transition is based on a time behavior described using the delay function in each cell. Exposed, Infection, Asymptomatic and Recovered states have a defined number of days that a population can be within the state before transitioning to the next this is defined by *Te, Ti, Tai* and *Tr*. The set of days within each state is described as $q = \{1, 2, \ldots, Tstate\}$. For example, $E_{i,a}^{t}(q)$, describes the proportion of exposed cases for an age group a in cell i at time t in exposed state $q = \{1, 2, \ldots, Te\}$. Our model includes k unique geographical cells. The proportion of a given population's age group a found in each state is described as: $S_{i,a}^{t}, E_{i,a}^{t}, A_{i,a}^{t}, I_{i,a}^{t}, R_{i,a}^{t}, D_{i,a}^{t}$ (cell i at time t for age group a). Each transition is built using the Cell-DEVS transition and delay functions, which implement equations 1 – 12 below.

Let us consider $fa(q)$ as the fatality rate of infected stage q for age group a; $\lambda a(q)$ their infection rate; $\mu a(q)$ their mobility rate; $\varepsilon a(q)$ the incubation rate; $\gamma a(q)$ the recovery rate and φ as the asymptomatic infection rate. Then, c_{ij} is the geographical correlation factor between cells i and j; k_{ij} is the correction factor applied to both cells i and j to model disobedience. Equation (1) calculates the proportion of deaths at time t as the total of current deaths plus the sum of the infectious population that died the day before. New deaths are equal to the newly deceased population moving from the infectious state multiplied by the fatality rate. The deceased transition does not consider asymptomatic infections as they do not lead to deaths.

$$D_{i,a}^{t+1} = D_{i,a}^{t} + \sum_{q=1}^{Ti} fa(q)\left(I_{i,a}^{t}(q)\right) \tag{1}$$

Equation (2) is used to calculate the proportion of the newly exposed population. This is calculated as the result of the susceptible ones in contact with either the entire infectious population or the asymptomatic population of neighboring cells j.

$$E_{i,a}^{t+1}(1) = S_{i,a}^{t}\sum_{j=1}^{k}\left(c_{ij}k_{ij} * \sum_{p\in\{1,2,\ldots,T_i\}}^{b\in A}\frac{N_{j,b}}{N_j}\mu_b(p)\lambda_{mask,b}^{t}(p)I_{j,b}^{t}(p)\right) + \left(c_{ij} * \sum_{p\in\{1,2,\ldots,T_i\}}^{b\in A}\frac{N_{j,b}}{N_j}\mu_b(p)\lambda_{mask,b}^{t}(p)Ai_{j,b}^{t}(p)\right) \tag{2}$$

The first part of the equation calculates the proportion of a cell's susceptible population exposed to an infectious individual (I) and the second part the proportion exposed to an asymptomatic individual (Ai). A defines the set of age groups in cell j, each age group is represented by b. The λ_{mask} is the infection rate after masks are considered, as in equations (4-6). Each cell's population represented by N_j is divided into age groups (subscript b). Each cell is related to its neighbor by a geographical correlation factor c_{ij} that describes the impact each neighboring cell has on a given cell, including infection rate and mobility rates a given cell's population has with its neighbors. Finally, k_{ij} defines a correction factor between cells i and j, applied to the infectious half of the equation to simulate infectious and asymptomatic populations: asymptomatic individuals are more carefree, thus they will expose more individuals (Del Valle et al. 2005). The correction factor k_{ij} is defined using the model disobedience factor d where $k_{ij}=min(k_i, k_j)$. The correction for individual cells i and j is defined as $k_{cell}=d+(1-d)*m_c$. The infection correction factor mc is defined in the model as a function of the ICU threshold (I_{TH}) that triggers a specific mobility correction factor (cm) and a removal level (R). Over time, the correction factor (cm) of a given cell can change due to lockdown fatigue.

We added lockdown fatigue to define the impact long lockdowns have on behavior and infection case counts. We have incorporated lockdown fatigue by calculating the time each geographical region has been

under lockdown and then checking if the time meets certain time requirements defined as in (Joshi and Musalem (2021): lockdown fatigue sets in after 28 days 30% of the lockdown impacts are gone, and after 121 days 100% are gone. These rates are based on previous research, and our model allows them to be modified to meet new research results easily Equation (3) shows how to calculate this lockdown effect.

$$cm = \begin{cases} cm, & L_t < 28 \\ 1 - ((1 - cm) * (1 - 0.301)), & L_t \geq 28 \; and \; L_t < 121 \\ 1.0, & L_t \geq 121 \end{cases} \tag{3}$$

The lockdown effect *cm* is based on the number of days a given cell has been in lockdown (L_t) and follows (Joshi and Musalem 2021), as discussed above. If a cell is under lockdown for less than 28 days *cm* has full effect. If a state is in lockdown, L_t is incremented. It is not enough to assume one day out of lockdown is enough to reset a population's behavior; hence, if a state comes out of lockdown, L_t is slowly lowered back to 0 where the population will behave normally again. This allows for the model to address the effect multiple lockdowns that may occur in quick succession have on a population's behavior.

Mask wearing was added to represent the impact masks have on infection transmission dynamics over time. This has been added as a modifier to the infection rate of the disease, using mask compliance and efficiency factors, which can be adjusted. The model also allows to define a "mask recommendation time" where the model can simulate the impact a mask mandate would have on rising case counts. In our case this is defined by applying the mask modifier after a given time. For example, if infection rate is 1.0, mask efficiency is 0.5, mask compliance is 0.5 and a mask recommendation time is set to 50 days, the infection rate would remain at 1.0 for the first 49 days, and on the 50th day the infection rate would begin lowering to 0.75 (equation 6). This equation defines a dynamic modified logistic regression function where the impact of masks can change over time depending on government restrictions.

$$\Lambda_{comp} = 1 - \left(\lambda * \left(mask_{eff} * mask_{comp}\right)\right) \tag{4}$$

$$\Lambda_{non-comp} = \lambda_{comp} * mask_d \tag{5}$$

$$\Lambda_{mask}(t) = \frac{\lambda - \lambda_{comp}}{1 + e^{-k_1(-t+t_1)}} + \frac{\lambda - \lambda_{non-com}}{1 + e^{-k_2(-t+t_2)}} + \lambda_{non-comp} \tag{6}$$

First, λ_{comp}(4) defines the infection rate for mask compliance, where $mask_{eff}$ and $mask_{comp}$ are the mask efficiency and mask compliance respectively. Mask efficiency can be modified to represent different types of masks. For example if infection rate (λ) is 1.0, mask efficiency ($mask_{eff}$) is 0.5 and mask compliance ($mask_{comp}$) is 0.7, our new infection rate (λ_{comp}) would be 0.65. $\lambda_{non-comp}$(5) defines the proportion of mask wearers who decide to not wear masks ($mask_d$) after government rules change. k_1 and k_2 define the rate at which the population begins mask wearing (k_1) or mask removal (k_2). t is the current day of the simulation; t_1 defines the day when government restrictions or lockdowns begin and t_2 defines the day when the restrictions are lifted. In our model t_1 and t_2 are set dynamically, as the simulation runs and new restrictions are declared t_1 is set on that day, while t_2 is an arbitrary date in the future. When restrictions are lifted t_2 is set, and the population will begin removing their masks. The model also allows for users to enter a mask recommendation time, if this is set, t_1 will be assigned to that day and the population will be given a mask recommendation when that day is reached.

Equation (7) describes how the exposed population transitions to the infectious or asymptomatic state. The equation defines the exposed in stage q is equal to the exposed of the previous day multiplied by $1-\varepsilon_a(q-1)$. Where $\varepsilon_a\,(q-1)$ defines the incubation rate for an age group a for state $q-1$. The incubation rate defines the probability of the population moving to infectious or asymptomatic.

$$E_{i,a}^{t+1}(q) = \left(1 - \varepsilon_a(q-1)\right)E_{i,a}^{t+1}(q-1), q \in (2, 3, \ldots, T_e) \tag{7}$$

Equation (8) describes the new infectious population that will occupy day 1. The equation considers the exposed population from all stages, and all age groups. As defined above in (7), a proportion of the

exposed population moves to infectious or asymptomatic based on the incubation rate ε_a. The rate at which the exposed population becomes either infectious, or asymptomatic is defined by asymptomatic rate φ. Thus, for the case of new infectious population the rate is defined as (1 – φ).

$$I_{i,a}^{t+1}(1) = E_{i,a}^{t}(T_e) + \sum_{q=1}^{Te-1}\left(\varepsilon_a(q)E_{i,a}^{t}(q)\right)(1-\varphi) \tag{8}$$

Equation (9) describes the portion of the infected population that moves to the next stage. The infectious population for stage q equals the population of infectious in the previous stage, $q - 1$ minus the population who move to either recovery or deceased. The portion of the population that move to the recovered or deceased states is defined by recovery rate γ and fatality rate f respectively.

$$I_{i,a}^{t+1}(q) = I_{i,a}^{t}(q-1) * \big(1-\gamma_a(q-1)-fa(q-1)\big), q \in (2,3,\dots,T_i) \tag{9}$$

Equations (10 and 11) define the asymptomatic state behavior following the same rules described in (8) and (9). Equation (10) defines the proportion of the exposed population that moves to the asymptomatic state (here, the asymptomatic population rate remains as φ). Equation (11) follows the same rules defined when asymptomatic cases either move to the next stage q or recovered.

$$A_{i,a}^{t+1}(1) = E_{i,a}^{t}(T_e) + \sum_{q\in\{1,2,\dots,T_e-1\}}(\varepsilon_a(q)E_{i,a}^{t}(q))\varphi \tag{10}$$

$$A_{i,a}^{t+1}(q) = A_{i,a}^{t}(q-1) * \big(1-\gamma_a(q-1)\big), q \in (2,3,\dots,T_{ai}) \tag{11}$$

Equation (12) describes the proportion of infectious or asymptomatic that recover. The number of recoveries is the total number of recoveries from the previous day plus the newly recovered population. The current day recoveries are calculated by taking the proportion of infectious and asymptomatic that move to the recovered stage using rate γ. Finally, we check individuals on the final day of either infectious or asymptomatic; they can move to the deceased state, or they are added to the recovered state.

$$R_{i,a}^{t+1}(1) = \left(I_{i,a}^{t}(T_i) + A_{i,a}^{t}(T_{ai})\right) + \sum_{q\in\{1,2,\dots,T_i-1\}}\gamma_a(q)I_{i,a}^{t}(q) + \sum_{q\in\{1,2,\dots,T_{ai}-1\}}\gamma_a(q)A_{i,a}^{t}(q) \tag{12}$$

Equations (13 and 14) are used only if re-susceptibility is not enabled. Once the recovered population reaches the final day of recovery, they remain there for the rest of the simulation time.

$$R_{i,a}^{t+1}(q) = R_{i,a}^{t}(q-1), q\epsilon\{2,3,\dots,T_r-1\} \tag{13}$$

$$R_{i,a}^{t+1}(T_r) = R_{i,a}^{t}(T_r) + R_{i,a}^{t}(T_r-1) \tag{14}$$

Equation (15) is an equation only used when re-susceptibility is enabled, i.e., patients who are recovered will go through each day of recovery, when they reach the final day of recovery the population will move back into the susceptible population pool where they can be re-exposed. The length of the recovery state represents the amount of time the population is naturally immune to the disease.

$$R_{i,a}^{t+1}(q) = R_{i,a}^{t}(q-1), q\epsilon\{2,3,\dots,\ T_r\} \tag{15}$$

Equation (16) is needed for the integrity. Since we know that any given population starts in the susceptible state, the population that is not in any other state should remain susceptible

$$S_{i,a}^{t+1} = 1 - \sum_{q=1}^{T_e}E_{i,a}^{t+1}(q) - \sum_{q=1}^{T_i}I_{i,a}^{t+1}(q) - \sum_{q=1}^{Tai}A_{i,a}^{t+1}(q) - \sum_{q=1}^{Tr}R_{i,a}^{t+1}(q) - D_{i,a}^{t+1} \tag{16}$$

The model is defined as a coupled Cell-DEVS where the space represents a geographical region, and each cell is a location using an irregular topology. Each cell consists of a cell ID, a set of state variables, a model configuration, and neighboring cell's correlation factors. The cell and atomic model where the states change within each cell independently of the neighbors, but the neighboring cells impact each other based on the correlation factor in Figure 1. Each atomic model has a population that begins as Susceptible; and then transitions through the other states based on the equations. The model implements each equation for any given number of geographical cells the user defines.

4 MODEL IMPLEMENTATION

The equations above are implemented; when all the geographical cells are defined, they are placed into a top level coupled cell model called *geographical_coupled*, with configuration seen in Figure 3. At runtime, the *geographical_coupled* model is initialized using cells data provided from in a JSON input file this is doing using the methods described in the top model class *cadmium::celldevs:cells_coupled<T,C,S,V>*; Figure 3 below describes how this coupled cell model is defined.

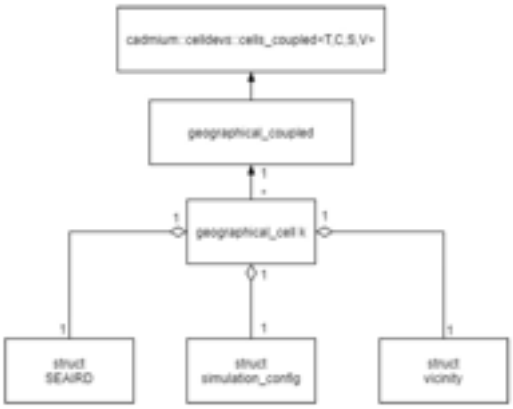

Figure 3: Coupled SEAIRD cell diagram.

At runtime, the *geographical_coupled* model is initialized using the cell's unique data. The cell's data is provided from a JSON input file using the methods described in the top model class *cadmium::celldevs:cells_coupled<T,C,S,V>;* Figure 3 shows how this coupled cell model is defined. The structures *SEAIRD*, *simulation_config* and *vicinity* define the inputs of *geographical_cell k*. *SEAIRD* defines the state variables used to hold the population, infection correction, disobedience factors, lockdown fatigue modifiers and mask wearing. The simulation configuration defines the attributes that characterize the disease being modelled including infection rates, incubation rates, fatality rates and asymptomatic rates. The vicinity structure holds the information defining the correlation factors between two geographical cells. These structures are read in at run time to create the single parameterized model *geographical_cell*. The *geographical_coupled* model is defined by the collection of geographical cells and their relationships.

In Figure 4 the relevant *SEAIRD* information is defined. Each cell has a unique population divided into age groups. The cell's population is divided into one of six states. When modeling the beginning of a pandemic, a single cell is assigned as the starting location; in this cell a small population will be infected or exposed, the remaining population will be susceptible. In this scenario, all other cells will have 100% of their population as susceptible. Our model allows users to define how the models parameters are defined. If needed the user can have the model start at any time point during the pandemic.

```
struct seaird {
    std::vector<double> age_group_proportions;
    std::vector<double> susceptible;
    std::vector<std::vector<double>> exposed;
    std::vector<std::vector<double>> infected;
```

```
    std::vector<std::vector<double>> asymptomatic;
    std::vector<std::vector<double>> recovered;
std::vector<double> fatalities;
std::unordered_map<std::string, lockdown_factor> lockdown _factors;
    double population;
    std::vector<double> disobedient;
    double days_in_lockdown;
    double mask_efficency;
    double mask_compliance;...};
```

Figure 4: SEAIRD configuration code.

In Figure 5 the simulation configuration is defined. These variables define how the population moves from one state to another. These variables also describe the disease that is being modelled, the transmission rates, incubation rates and the other important variables that describe how a disease behaves. The structures shown above define the *geographical_cell* atomic model shown in Figure 3. A *geographical_cell* atomic model is defined for each unique geographical cell in the model, where the collection of these atomic models make the geographical_coupled model. Finally, the *geographical_coupled* model is defined by the methods found in class *cadmium::celldevs::cells_coupled<T,C,S,V>*.

```
struct simulation_config {
    int prec_divider;
    using phase_rates = std::vector<std::vector<double>>;
    phase_rates infection_rates;
    phase_rates incubation_rates;
    phase_rates recovery_rates;
    phase_rates mobility_rates;
    phase_rates fatality_rates;
    double asymptomatic_rates;
    bool SIIRS_model = true; };
```

Figure 5: Simulation configuration code.

5 PROVINCIAL COVID-19 SPREAD

In this section we use the SEAIRD discussed above to execute different simulation scenarios generated using data collected from the Canadian Provinces. The results in this section will compare the different effects human behavior has on mask wearing, lockdown fatigue and how different government restrictions can change the trajectory of the pandemic using Statistics Canada census data (Statistics Canada 2021).

The parameters used in this study are described in Table 1:

Table 1. Test case configuration.

Parameter	**Value**
Population	Varies per cell, based on Canada census data
Age Groups	Varies per cell, based on Canada census data
Disobedience Rates	[0.29, 0.25, 0.23, 0.21, 0.24]
Asymptomatic Rate	Varies per simulation (See figure descriptions)
Infection Rate	0.6 across all states and age groups
Incubation Time	14-day profile (Davidson and Wainer 2021)
Mobility Rates	1.0 across all states and age groups
Recovery Rates	0.07 across all states and age groups
Fatality Rates	0.005 across all states and age groups
ICU correction factors (lockdown/restrictions)	0.5: [0.25, 0.3],0.75: [0.25, 0.1] ,1.0: [0.005, 0.05]
Mask efficiency	Varies per simulation (See figure descriptions)
Mask compliance	Varies per simulation (See figure descriptions)
Mask policy onset times	Varies per simulation (See figure descriptions)

We have a population defined for each geographical area. Then we use the vector of age group values to split the population into the correct age group proportions. Our age group values were gathered using Canadian census data where our values represent the following five age groups: 0-14, 15-19, 20-44, 45-65, and over 65 years old. Disobedience follows the same format where each value represents a proportion of the age group that disobey restrictions; this is estimated using data gathered by the Angus Reid Institute (2020) and Carlucci et al. (2020). "All states and age groups" means that the value shown is the same for each state of disease transmission and the same across all age groups. Incubation time is the number of days a population is exposed before becoming infected or asymptomatic; this is defined using a 14-day profile where each day the population has a chance to move to the next state (Davidson and Wainer 2021). Mobility rates define the population movement; 1.0 means there are no mobility restrictions. Recovery rates are the rate at which the population can recover from the disease, 0.07 means for each day the population is infected, they have a 7% chance to recover. Fatality rates define the chance the population will die on a given day of the infection. ICU correction factor describe the proportion of the population that is estimated to be in the ICU before government restrictions are required. This value is estimated based on the number of infectious individuals. ICU capacity is unique to each geographical region, the ICU capacity data was gathered using data gathered from (Fowler et al. 2015). The values shown for the ICU correction factor can be described as: 'Proportion of population infected to start restrictions': ['mobility modifier', 'Proportion of population infected to lift restrictions'] where mobility modifier reduces the mobility of a cell by the given value. The mobility modifier can change over time (equation 6). Mask efficiency and compliance are tested using differing values based on a number of studies that shown the difference between surgical, cloth, or N95 masks (Grinshpun et al. 2009; Rengasamy et al. 2014; Willeke et al. 1996).

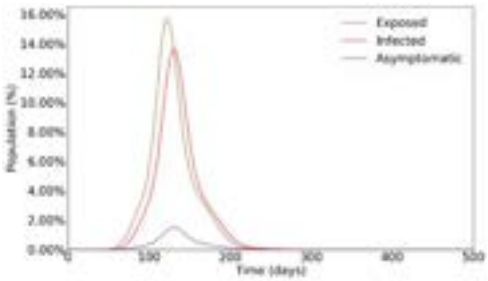

Figure 6: Base line – No masks worn, 10% asymptomatic.

In Figure 6 we see a single wave with a steep curve. The population becomes exposed rapidly, and then 1-14 days after exposure, they become infected. The total infected reaches 14% of the population, causing to require a hard lockdown to bring the infected count back down. No mask wearing has been enabled, and the re-susceptibility field has been set to false. Due to the lack of mask wearing, the infectivity rate is left at its full value, this leads to cases spreading at a fast rate. Instead, Figure 7 shows the same scenario but now 75% of the population is wearing a mask, the masks have 50% efficiency at reducing transmissions and the population is given a mask mandate after 50 days.

We can see the population becomes infected more slowly, ideally giving the government more time to plan and act. The peak of cases is also much lower with only 7% of the entire population becoming infected; 50% less than in Figure 6. This allows for some of the restrictions to be lifted leading to cases slowly returning to 0. We can see that around day 260 the infected begin dropping slower, due to lockdown fatigue starting to set in. As described in equation 3 the model detects that some of the cells within the simulation have been in lockdown for weeks around day 260, thus increasing the mobility within the cell and the neighboring cells. Around this time cases have dropped enough for restrictions to begin loosening as well, with less restrictions the population begins believing they are safe, this will cause some of the population to start removing their masks, slightly increasing the infectivity again. If re-susceptibility were enabled in the model, cases would begin climbing again at this point. This can be seen in more detail in Figure 8.

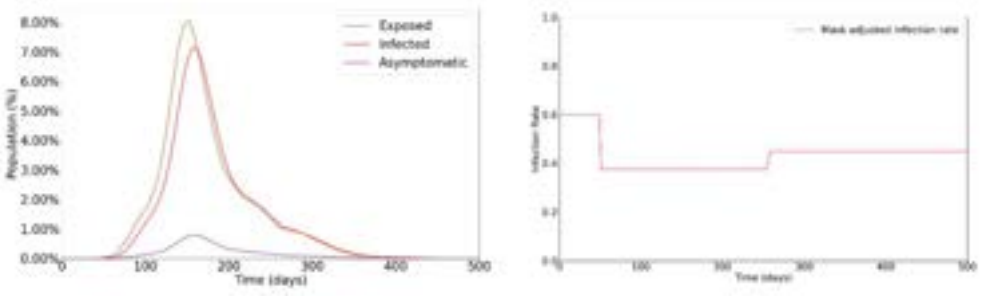

Figure 7: 50% Mask efficiency, 75% mask compliance, 10% asymptomatic, 50-day mask requirement (left). Mask adjusted infection rate over time (right).

In Figure 8 we can see the same scenario as Figure 7, but now re-susceptibility has been enabled. We can see that the first wave trajectory is the same as figure 7, but now when government restrictions begin to lower, and lockdown fatigue rising, a second wave begins. Due to the lingering lockdown fatigue, the second wave ends up with slightly more cases than the first wave. At the end of the second wave, government restrictions start lifting, we can see (right) that some of the population begin removing their masks, causing the infection rate to rise once again. The rise of cases at the end of the model's runtime causes new government restrictions to be applied, this can be seen by mask wearing resuming in figure 8 (right). This rise in infection rate shows the start of what would be a third wave. From the models point of view, when a given cell lockdown ends, some of the masked population believe they are safe to begin removing masks. This leads to the increase and decrease in infection rate shown. Although lockdowns are lifted mask mandates may not have ended yet, this allows for the model to simulate how changes in government policy can indirectly impact disease spread due to how the population perceives the change.

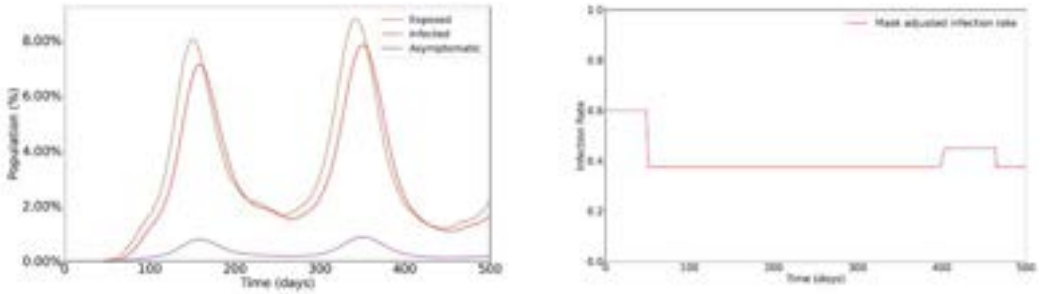

Figure 8: 50% Mask efficiency, 75% mask compliance, 10% asymptomatic, 50-day mask requirement, with re-susceptibility enabled (left) Mask adjusted infection rate over time (right).

In Figure 9 we can see an example of the geographical visualization for our scenario. The visualizer (St-Aubin et al. 2018) allows for animation showing a timeline of the pandemic (day 111). In this scenario, the first case was in Ontario, thus the provinces connected to Ontario (Manitoba, Quebec) have more cases at this time than further provinces such as British Columbia and Yukon. Due to the correlation factor being based on border length, places with very few or small land borders get less cases, as seen when examining Nova Scotia. When comparing to Figure 8 we can see that at day 111 the disease was spreading rapidly but had not hit the yet. We can understand the geographical transmission dynamics behind the curve showing how the disease spread fastest in certain provinces and slower in others. The visualization allows users to select different layers, this can be used to view other model parameters like days in lockdown showing how different provinces healthcare capacities allowed them to remove lockdowns earlier than others.

With these results being shown, our model has the capability to simulate the impact human behaviors around masks and lockdown fatigue has on case counts. The model shows how early mask mandates slow the rise of infections, and overall lower the number of infections throughout the population. We can model

how a population might perceive lowered restrictions as a sign they can remove their masks. The model will also allow the simulation of lockdown fatigue, showing how longer lockdowns can cause slower decline in cases over time or cause second waves that infect more than the first wave.

Figure 9: Geographical visualization.

6 CONCLUSIONS & FUTURE WORK

We presented a model that allows users to create rapid simulation prototypes to simulate the impact different human behaviors have on disease spread. The model was built to simulate COVID-19 spread but has the ability to change for any other disease a user requires. The design of the model allows for quick, efficient prototyping where users can change mask wearing, asymptomatic rates, or government restrictions with ease. Users simply need to update the disease or population information, regenerate the population, and run the model. The model shows results where re-susceptibility, mask mandates, mask wearing over time and lockdown fatigue are present.

Future adaptations of the model could incorporate new methods of geographical disease spread where information like traffic movement, and flight travel are incorporated. The model could be further adapted to include new states and transitions. In future adaptations variants of concerns and disease mutations can be addressed allowing for the simulation of multiple disease types.

REFERENCES

Angus Reid Institute. 2020. “COVID-19 Compliance: One-in-Five Canadians Making Little to No Effort to Stop Coronavirus Spread.” http://angusreid.org/covid-compliance/, accessed 10th March 2023.

Calafiore, G. C., N. Carlo and P. Corrado 2020. “A Time-Varying SIRD Model for the COVID-19 Contagion in Italy.” *Annual Reviews in Control* 50:361–72.

Cárdenas, R, K. Henares, C. Ruiz-Martín, and G. Wainer. 2021. “Cell-DEVS Models for the Spread of COVID-19.” *International Conference on Cellular Automata for Research and Industry ACRI 2020.* December 2nd-4th, Lodz, Poland, 239-249.

Carlucci, L, I. D’ambrosio and M. Balsamo. 2020. “Demographic and Attitudinal Factors of Adherence to Quarantine Guidelines during Covid-19: The Italian Model.” *Frontiers in Psychology* 11:1–13.

Davidson, G and G. Wainer. 2021. “Studying COVID-19 Spread Using a Geography Based Cellular Model; Studying COVID-19 Spread Using a Geography Based Cellular Model.” *2021 Winter Simulation Conference (WSC)*, December 12th-15th, Phoenix, AZ, USA, 1-12.

Fahlman, A, C. Ruiz-Martin, G. Wainer, P. Dobias and M. Rempel. 2021. “EXTENDED COMPARTMENTAL MODEL OF COVID-19: A CELL-DEVS DEFITINION.” *2021 IEEE/ACM 25th International Symposium on Distributed Simulation and Real Time Applications (DS-RT)* , September 27th-29th, Valencia, Spain, 1-8.

Flaxman, S, S. Mishra, A. Gandy, H.J.T. Unwin, T.A. Mellan, H. Coupland, C. Whittaker, H. Zhu, T. Berah, J.W. Eaton, M. Monod, A.C. Ghani, C.A. Donnelly, S. Riley, M.A.C. Vollmer, N.M. Ferguson, L.C. Okell and S.Bhatt. 2020. “Estimating the Effects of Non-Pharmaceutical Interventions on COVID-19 in Europe." *Nature* 584(7820): 257–261.

Fowler, R.A, P. Abdelmalik, G. Wood, D. Foster, N. Gibney, N. Bandrauk, A.F. Turgeon, F. Lamontagne, A. Kumar, R. Zarychanski, R. Green, S.M. Bagshaw, H.T. Stelfox, R. Foster, P. Dodek, S. Shaw, J. Granton, B. Lawless, A. Hill, L. Rose,

N.K. Adhikari, D.C. Scales, D.J. Cook, J.C. Marshall, C. Martin and P.Jouvet. 2015. “Critical Care Capacity in Canada: Results of a National Cross-Sectional Study.” *Critical Care* 19(1): 133.

Giordano, G, F. Blanchini, R. Bruno, P. Colaneri, A.D. Filippo, A.D. Matteo and M. Colaneri. 2020. "Modelling the COVID-19 Epidemic and Implementation of Population-Wide Interventions in Italy" *Nature Medicine* 26:855-860.

Goldstein, P, E.L. Yeyati, and L Sartorio. 2021. “Lockdown Fatigue: The Diminishing Effects of Quarantines on the Spread of COVID-19.” *Harvard Working Papers* 391.

Grinshpun, S.A., H. Haruta, R.M. Eninger, T. Reponen, R.T. McKay and S. Lee. 2009. “Performance of an N95 Filtering Facepiece Particulate Respirator and a Surgical Mask during Human Breathing: Two Pathways for Particle Penetration.” *Journal of Occupational and Environmental Hygiene* 6(10):593–603.

Joshi, Y.V, and A. Musalem. 2021. “Lockdowns Lose One Third of Their Impact on Mobility in a Month.” *Nature Scientific reports* 11:22658.

Tay, B.K., C.A. Roby, J.W. Wu and D.Y. Tan. 2021. “Dynamical Analysis of Universal Masking on the Pandemic.” *International Journal of Environmental Research and Public Health* 18(17):9027.

Kermack, W.O, and A. G. McKendrick. 1927. “A Contribution to the Mathematical Theory of Epidemics.” *Proceedings of the Royal Society.* 115(772):700–721.

Korolev, I. 2021. “Identification and Estimation of the SEIRD Epidemic Model for COVID-19.” *Journal of Econometrics* 220(1):63–85.

Mader, A, and T. Rüttenauer. 2022. “The Effects of Non-Pharmaceutical Interventions on COVID-19 Mortality: A Generalized Synthetic Control Approach Across 169 Countries.” *Frontiers in Public Health* 10:1–8.

Maged, A, A. Ahmed, S. Haridy, A.W. Baker and M. Xie. 2022. “SEIR Model to Address the Impact of Face Masks amid COVID-19 Pandemic.” *Wiley Public Health Emergency Collection*. 43:129-143.

Mohammadi, Z, M.G. Cojocaru, and E.W. Thommes. 2022. “Human Behavior, NPI and Mobility Reduction Effects on COVID-19 Transmission in Different Countries of the World.” *BMC Public Health* 22(1594):1-19.

Oraby, T, M.G. Tyshenko, J.C. Maldonado, K. Vatcheva, S. Elsaadany, W.Q. Alali, J.C. Longenecker and M. Al-Zoughool. 2021. “Modeling the Effect of Lockdown Timing as a COVID-19 Control Measure in Countries with Differing Social Contacts.” *Nature Scientific Reports* 11(3354):1-13.

Organization, World Health. 2021. *WHO Coronavirus (COVID-19) Dashboard.* https://covid19.who.int/, accessed 12th March 2023.

Potasman, I. 2017. “Asymptomatic Infections: The Hidden Epidemic.” *International Journal of Clinical Research & Trials* 2:118.

Rengasamy, S, B.C. Eimer, and J. Szalajda. 2014. “A Quantitative Assessment of the Total Inward Leakage of Nacl Aerosol Representing Submicron-Size Bioaerosol through N95 Filtering Facepiece Respirators and Surgical Masks.” *Journal of Occupational and Environmental Hygiene* 11(6):388–396.

Sattenspiel, L, and K. Dietz. 1995. “A Structured Epidemic Model Incorporating Geographic Mobility among Regions.” *Mathematical biosciences* 128:71–91.

St-Aubin, B, O. Hesham, and G. Wainer. 2018. “A Cell-Devs Visualization and Analysis Platform.” *SummerSim-SCSC 2018*, July 9th-12th, Bordeaux, France, 157-168.

Statistics Canada. 2021. “Census of Canada: Profile Data for Canada.” *Census Profile, 2021 Census of Population*, accessed 12th March 2023.

Urrutia, D, E. Manetti, M. Williamson and E. Lequy. 2021. “Overview of Canada’s Answer to the COVID-19 Pandemic’s First Wave (January-April 2020).” *International Journal of Environmental Research and Public Health* 18(13):7131.

Del Valle, S., H. Hethcote, J. M. Hyman, and C. Castillo-Chavez. 2005. “Effects of Behavioral Changes in a Smallpox Attack Model.” *Mathematical Biosciences* 195(2):228–51.

Vicino, B, L. Belloli, C. Ruiz-Martin, and G.A. Wainer. 2019. “Building DEVS Models with the cadmium tool” In *Proceedings of the 2019 Winter Simulation Conference*, December 8th-11th, National Harbor. MD, USA, 45-59.

Wainer, G.A. 2014. “Cellular Modeling with Cell-DEVS: A Discrete-Event Cellular Automata Formalism.”*International Conference on Cellular Automata for Research and Industry*, September 22nd-25th, Krakow, Poland, 6–15.

Willeke, K, Y. Qian, J. Donnelly, S. Grinshpun and V. Ulevicius. 1996. “Penetration of Airborne Microorganisms through a Surgical Mask and a Dust/Mist Respirator.” *American Industrial Hygiene Association journal* 57(4):348–355.

Zeigler, B.P, H. Praehofer, and T.G. Kim. 2000. *Theory of Modeling and Simulation: Integrating Discrete Event and Continuous Complex Dynamic Systems*. San Diego, CA: Academic Press.

Zhong, S.B., Q. Huang, and D. Song. 2009. “Simulation of the Spread of Infectious Diseases in a Geographical Environment.” *Science in China, Series D: Earth Sciences* 52(4):550–561.

AUTHOR BIOGRAPHIES

AIDAN FAHLMAN has a Masters degree in Systems and Computer Engineering at Carleton University (Ottawa, ON, Canada). His email address is aidanfahlman@cmail.carleton.ca.

GABRIEL WAINER is a Professor at the Department of Systems and Computer Engineering at Carleton University (Ottawa, ON, Canada). He is a Fellow of SCS. His email address is gwainer@sce.carleton.ca.